

Research Article

Evasion-Pursuit Strategy against Defended Aircraft Based on Differential Game Theory

Qilong Sun ¹, Minghui Shen ¹, Xiaolong Gu ¹, Kang Hou ¹ and Naiming Qi ²

¹Beijing Institute of Space Long March Vehicle, Beijing 100076, China

²Harbin Institute of Technology, Harbin 100050, China

Correspondence should be addressed to Qilong Sun; sunqilong27@163.com

Received 16 October 2018; Accepted 15 January 2019; Published 12 March 2019

Guest Editor: Ernesto Staffetti

Copyright © 2019 Qilong Sun et al. This is an open access article distributed under the Creative Commons Attribution License, which permits unrestricted use, distribution, and reproduction in any medium, provided the original work is properly cited.

The active defense scenario in which the attacker evades from the defender and pursues the target is investigated. In this scenario, the target evades from the attacker, and the defender intercepts the attacker by using the optimal strategies. The evasion and the pursuit boundaries are investigated for the attacker when the three players use the one-to-one optimal guidance laws, which are derived based on differential game theory. It is difficult for the attacker to accomplish the task by using the one-to-one optimal guidance law; thus, a new guidance law is derived. Unlike other papers, in this paper, the accelerations of the target and the defender are unknown to the attacker. The new strategy is derived by linearizing the model along the initial line of sight, and it is obtained based on the open-loop solution form as the closed-loop problem is hard to solve. The results of the guidance performance for the derived guidance law are presented by numerical simulations, and it shows that the attacker can evade the defender and intercept the target successfully by using the proposed strategy.

1. Introduction

In the traditional pursuit-evasion scenario, the guidance law was investigated for two players which included an evasion target and a pursuit attacker. Zarchan studied a variety of guidance laws for this pursuit-evasion scenario [1]. A new impact time and angle control guidance law against stationary and nonmaneuvering targets was investigated for the missile [2]. A novel extended proportional guidance law was designed to intercept the maneuvering target [3]. The adaptive integral sliding mode guidance law was derived in a three-dimensional scenario [4, 5]. In these papers, the acceleration of the target was a known bounded external disturbance to the missile. A two-phase optimal guidance law was derived to improve the estimation accuracy and terminal performances for impact angle constraint engagement [6]. Yang et al. [7] presented a time-varying biased proportional guidance law in which two time-varying bias terms were applied to divide the trajectory into the initial phase and terminal phase. Recently, various pursuit-evasion scenarios involving multiple players have been investigated. The

guidance laws for two missiles attacking one target were analyzed [8, 9]. References [10–12] described a scenario in which multimissiles attacked one target, and the cooperative guidance laws were derived.

When a missile attacks the aircraft, the aircraft always launches a defender to protect itself. Meanwhile, the aircraft evades the attacking missile. The problem which includes a target aircraft, a defender, and an attacking missile is known as the active defense scenario. It is difficult for a missile to hit the aircraft that launched a defender by using the traditional guidance law. The three-player engagement is different from the typical one-to-one engagement. In recent years, the strategies in the active defense scenario have been a hot topic, and especially, the cooperative guidance laws between the target and the defender have been studied a lot.

A scenario in which the defender and the fixed or slowly moving target constituted the defended system was investigated [13–15]. In these papers, the optimal defense guidance laws were derived under the condition that the positions and the trajectories of the target and the attacker were known to the defender. Rusnak [16] investigated a scenario in which

the lady evaded from the bandit that pursued the lady and the body guard intercepted the bandit before the bandit captured the lady. In this paper, the optimal strategies were derived based on the differential game theory and optimal control theory. Line of sight (LOS) guidance law was investigated to intercept the attacker and protect the target [17]. In this paper, the defender is located on the line of sight of the attacker and the target. The defender could intercept the attacker with less control by using the LOS guidance law than by using the traditional guidance law. The cooperative optimal guidance laws between the target and the defender were studied [18–20]. In these papers, the target launched one defender, and the guidance laws were derived by differential game theory. The defender and the target helped each other to intercept the attacker. Oyler et al. [21] studied the pursuit-evasion games in the presence of obstacles that inhibited the motions of the players. The dominance regions were presented and analyzed to provide a complete solution to the game. Unlike previous research, two defenders were launched from the target to protect itself [22, 23]. In Reference [23], the cooperation between the defenders and the target was one-way which meant one defender received the information from the target and another defender sent information to the target. In Refs. [24–26], the cooperative guidance law for protecting the target was investigated by using nonlinear methods, and the defender could intercept the attacker with high heading angle errors. The conditions were investigated for the attacker winning the game in the active defense scenario by using the differential game theory [27]. Rubinsky and Gutman [28] investigated a three-player scenario in which the attacker evaded a defender and continued to pursue a target. In this scenario, the target and defender were independent, and the derived guidance law is only suited for the condition that the zero-effort-miss (ZEM) distance between the attacker and the target is not a large value. An evasion and pursuit guidance law for the attacking missile was analyzed [29], and the control efforts of the defender and the target were known to the attacking missile. In this paper, the attacking missile chose an appropriate lateral acceleration to maneuver before the defender and the attacking missile met, then the attacking missile used the optimal pursuit guidance law to hit the aircraft.

In the previous paper, the studies always focused on the cooperative guidance law between the aircraft and the defender. However, the attacking guidance law for the attacker winning the game is relatively rare. Refs. [27–29] presented the attacking guidance laws for the attacking missile. However, in these papers, the control efforts of the target and the defender were known to the missile, and they were hard to obtain in reality. The method presented in Reference [28] is unsuited for the condition that the zero-effort-miss (ZEM) distance between the attacker and the target is large, and the zero-effort-miss (ZEM) distance between the attacker and the defender is small.

In this paper, a new strategy is investigated for the attacker to hit the target. In this scenario, the miss distance between the target and the attacker and the miss distance between the defender and the attacker are considered for the attacker at the same time. The target and the defender

are independent, and they use the optimal strategies. It is not necessary for the attacker to obtain the control efforts of the target and the defender by using the derived guidance law.

2. Problem Formulation

The problem consists of three players: an attacker (A), a target (T), and a defender (D), and the scenario is described in Figure 1. LOS is the line of sight. R and V represent the range and velocity. γ represents the flight path angle. λ represents the angle between line of sight and the X axis. The lateral acceleration is denoted by α . The subscripts A, T, and D represent the corresponding players. AT and AD present the corresponding parameters between the players.

Neglecting the gravitational force, the geometric relations for the rates of the ranges are obtained by

$$\begin{aligned}\dot{R}_{AT} &= V_A \cos(\gamma_A - \lambda_{AT}) + V_T \cos(\gamma_T + \lambda_{AT}), \\ \dot{R}_{AD} &= V_A \cos(\gamma_A - \lambda_{AD}) + V_D \cos(\gamma_D + \lambda_{AD}).\end{aligned}\quad (1)$$

The LOS rate relations are expressed as follows:

$$\begin{aligned}\dot{\lambda}_{AT} &= \frac{V_T \sin(\gamma_T + \lambda_{AT}) - V_A \sin(\gamma_A - \lambda_{AT})}{R_{AT}}, \\ \dot{\lambda}_{AD} &= \frac{V_D \sin(\gamma_D + \lambda_{AD}) - V_A \sin(\gamma_A - \lambda_{AD})}{R_{AD}}.\end{aligned}\quad (2)$$

The dynamics of each player are considered to be a linear time-invariant system that can be described by the following equations [24]:

$$\begin{aligned}\dot{\delta}_{n \times 1}^i &= \alpha_{n \times n}^i \delta_{n \times 1}^i + \beta_{n \times 1}^i u_p^i \quad i = \{A, T, D\}, \\ \alpha_i K_{1 \times n}^i \delta_{n \times 1}^i + d_i u_p^i & \quad i = \{A, T, D\}.\end{aligned}\quad (3)$$

Here, δ_i is the state vector of internal state variables of each agent with $\dim(\delta_i) = n_i$, and u_p^i represents its controller.

The path angle relations satisfy the following equation:

$$\dot{\gamma}_i = \frac{a_i}{V_i}, \quad i = \{A, T, D\}.\quad (4)$$

It is assumed that the problem occurs in the endgame phase and the defender separates from the target; thus, the problem can be linearized along the initial lines of sight. The relative displacement between two players normal to LOS_0 is denoted as $y_i \{i = AT, AD\}$. The accelerations of the attacker and target normal to LOS_{AT} are denoted by $u_{AL_{AT}}$ and $u_{TL_{AT}}$. The acceleration of the defender normal to LOS_{AD} is defined by $u_{DL_{AD}}$. Thus, we can obtain

$$\begin{cases} \ddot{y}_{AT} = u_{TL_{AT}} - u_{AL_{AT}}, \\ \ddot{y}_{AD} = u_{DL_{AD}} \mathbf{\Gamma}(t) - \kappa u_{AL_{AT}}, \end{cases}\quad (5)$$

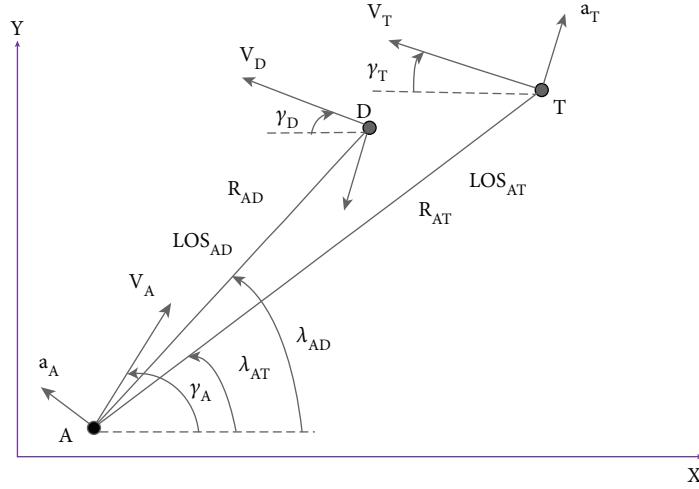


FIGURE 1: Engagement geometry.

where

$$\begin{cases} u_{AL_{AT}} = a_A \cos(\gamma_A - \lambda_{AT}) = (K_{1 \times n}^A x_A + d_A u_A') \cos(\gamma_A - \lambda_{AT}), \\ u_{TL_{AT}} = a_T \cos(\gamma_T + \lambda_{AT}) = (K_{1 \times n}^T x_T + d_T u_T') \cos(\gamma_T - \lambda_{AT}), \\ u_{DL_{AD}} = a_D \cos(\gamma_D + \lambda_{AD}) = (K_{1 \times n}^D x_D + d_A u_D') \cos(\gamma_D - \lambda_{AD}), \end{cases}$$

$$\Gamma(t) = \begin{cases} 1, & t < t_f^{AD}, \\ 0, & t \geq t_f^{AD}, \end{cases}$$

$$\kappa = \frac{\cos(\gamma_A - \lambda_{AD})}{\cos(\gamma_A - \lambda_{AT})}.$$
(6)

We solve the problem under the condition that the players A, T, and D obey ideal dynamics. Thus, $a_{n \times n}^i, \beta_{n \times 1}^i, K_{1 \times n}^i = 0, d_i = 1$. It can be obtained by

$$\begin{cases} u_{AL_{AT}} = a_A \cos(\gamma_A - \lambda_{AT}) = u_A' \cos(\gamma_A - \lambda_{AT}), \\ u_{TL_{AT}} = a_T \cos(\gamma_T + \lambda_{AT}) = u_T' \cos(\gamma_T + \lambda_{AT}), \\ u_{DL_{AT}} = a_D \cos(\gamma_D + \lambda_{AD}) = u_D' \cos(\gamma_D + \lambda_{AD}). \end{cases} \quad (7)$$

$u_A, u_T,$ and u_D satisfy the following form:

$$\begin{cases} u_A = u_A' \cos(\gamma_A - \lambda_{AT}), \\ u_T = u_T' \cos(\gamma_T + \lambda_{AT}), \\ u_D = u_D' \cos(\gamma_D + \lambda_{AD}). \end{cases} \quad (8)$$

The state vector of the linearized engagement is expressed as follows:

$$x = [\gamma_{AT} \quad \dot{\gamma}_{AT} \quad \gamma_{AD} \quad \dot{\gamma}_{AD}]^T. \quad (9)$$

The equations of motion corresponding to equation (9) are given by

$$\dot{x} = \begin{cases} \dot{\gamma}_{AT} = x_2, \\ \ddot{\gamma}_{AT} = u_T - u_A, \\ \dot{\gamma}_{AD} = x_4, \\ \ddot{\gamma}_{AD} = u_D \Gamma(t) - \kappa u_A. \end{cases} \quad (10)$$

The equations can be written in the following form:

$$\dot{x} = Ax + B[u_T \quad u_D]^T + Cu_A, \quad (11)$$

where

$$A = \begin{bmatrix} 0 & 1 & 0 & 0 \\ 0 & 0 & 0 & 0 \\ 0 & 0 & 0 & 1 \\ 0 & 0 & 0 & 0 \end{bmatrix},$$

$$B = \begin{bmatrix} 0 & 0 \\ 1 & 0 \\ 0 & 0 \\ 0 & \Gamma(t) \end{bmatrix}, \quad (12)$$

$$C = \begin{bmatrix} 0 \\ -1 \\ 0 \\ -\kappa \end{bmatrix}.$$

The intercept times are considered to be fixed because of the problem occurring in the endgame phase, and they can be given by

$$\begin{cases} t_f^{AT} = \frac{R_{AT_0}}{V_{A_0} \cos(\gamma_{A_0} - \lambda_{AT_0}) + V_{T_0} \cos(\gamma_{T_0} + \lambda_{AT_0})}, \\ t_f^{AD} = \frac{R_{AD_0}}{V_{A_0} \cos(\gamma_{A_0} - \lambda_{AD_0}) + V_{D_0} \cos(\gamma_{D_0} + \lambda_{AD_0})}. \end{cases} \quad (13)$$

After t_f^{AD} , the defender will disappear. The time-to-go t_{go} can be described by

$$t_{go}^i = t_f^i - t, \quad i = \{AT, AD\}. \quad (14)$$

3. Strategy for the Attacker

3.1. Order Reduction. The order of the problem needs to be reduced so that it can be solved expediently. The well-known zero-effort-miss (ZEM) distance between the attacker and the target can be expressed as follows:

$$Z_{AT}(t) = D_{AT} \Phi(t_f^{AT}, t) x. \quad (15)$$

Similarly, the ZEM distance between the attacker and the defender can be expressed as follows:

$$Z_{AD}(t) = D_{AD} \Phi(t_f^{AD}, t) x, \quad (16)$$

where $\Phi(t_f^{AT}, t)$ and $\Phi(t_f^{AD}, t)$ are the transition matrices with respect to equation (11),

$$\begin{cases} \dot{\Phi}(t_f^{AD}, t) = -\Phi(t_f^{AD}, t) A, \Phi(t_f^{AD}, t_f^{AD}) = \mathbf{I}, \\ \dot{\Phi}(t_f^{AT}, t) = -\Phi(t_f^{AT}, t) A, \Phi(t_f^{AT}, t_f^{AT}) = \mathbf{I}. \end{cases} \quad (17)$$

D_{AD} and D_{AT} are expressed as follows:

$$\begin{cases} D_{AD} = [0 & 0 & 1 & 0], \\ D_{AT} = [1 & 0 & 0 & 0]. \end{cases} \quad (18)$$

Equations (15) and (16) can be presented by

$$\begin{cases} Z_{AD}(t) = y_{AD} + \dot{y}_{AD}(t_f^{AD} - t), \\ Z_{AT}(t) = y_{AT} + \dot{y}_{AT}(t_f^{AT} - t). \end{cases} \quad (19)$$

The dynamics of $Z_{AT}(t)$ and $Z_{AD}(t)$ can be obtained by

$$\begin{cases} \dot{Z}_{AD}(t) = (t_f^{AD} - t)(-\kappa u_A + \mathbf{\Gamma}(t) u_D), \\ \dot{Z}_{AT}(t) = (t_f^{AT} - t)(-u_A + u_T). \end{cases} \quad (20)$$

3.2. One-to-One Optimal Strategies. In the attacker-target engagement, the attacker needs to pursue the target. The cost function to solve the problem is expressed by

$$J_{AT} = \frac{1}{2} [y_{AT}(t_f^{AT})]^2. \quad (21)$$

Because of $y_{AT}(t_f^{AT}) = Z_{AT}(t_f^{AT})$, the cost function can be rewritten in the following form:

$$J_{AT} = \frac{1}{2} [Z_{AT}(t_f^{AT})]^2. \quad (22)$$

Similarly, in the attacker-defender engagement, the attacker needs to evade from the defender. The cost function to solve the problem is expressed by

$$J_{AD} = -\frac{1}{2} [Z_{AD}(t_f^{AD})]^2. \quad (23)$$

The Hamiltonian functions corresponding to equations (23) and (22) are given by

$$\begin{cases} H_{AD} = \lambda_1 \dot{Z}_{AD}(t), \\ H_{AT} = \lambda_2 \dot{Z}_{AT}(t). \end{cases} \quad (24)$$

The adjoint equation and transversality condition are as follows:

$$\begin{cases} \dot{\lambda}_1 = -\frac{\partial H}{\partial Z_{AD}} = 0, \quad \lambda_1(t_f^{AD}) = \frac{\partial J_{AD}}{\partial Z_{AD}(t_f^{AD})} = -Z_{AD}(t_f^{AD}), \\ \dot{\lambda}_2 = -\frac{\partial H}{\partial Z_{AT}} = 0, \quad \lambda_2(t_f^{AT}) = \frac{\partial J_{AT}}{\partial Z_{AT}(t_f^{AT})} = Z_{AT}(t_f^{AT}). \end{cases} \quad (25)$$

Thus, the solution can be obtained as follows:

$$\begin{cases} \lambda_1(t) = -Z_{AD}(t_f^{AD}), \\ \lambda_2(t) = Z_{AT}(t_f^{AT}). \end{cases} \quad (26)$$

Substituting equations (26) and (20) into equation (24), it can be obtained in the following form:

$$\begin{cases} H_{AD} = -Z_{AD}(t_f^{AD})(t_f^{AD} - t)(-u_A \kappa + \mathbf{\Gamma}(t) u_D), \\ H_{AT} = Z_{AT}(t_f^{AT})(t_f^{AT} - t)(-u_A + u_T). \end{cases} \quad (27)$$

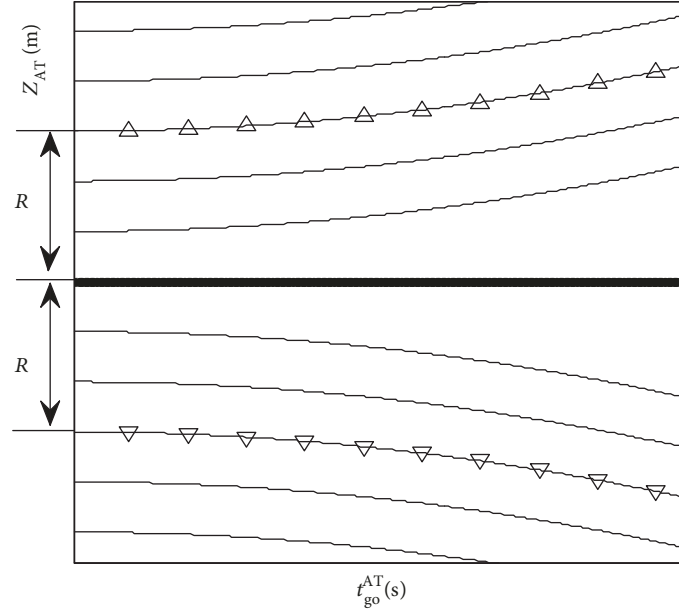


FIGURE 2: Optimal pursuit trajectories.

The optimal strategies for the attacker-target engagement are as follows:

$$\begin{cases} u_A^\ominus = \text{sign}(Z_{AT}(t))u_A^{\max}, \\ u_T^\ominus = \text{sign}(Z_{AT}(t))u_T^{\max}. \end{cases} \quad (28)$$

The optimal strategies for the attacker-defender engagement are as follows:

$$\begin{cases} u_A^\ominus = -\text{sign}[Z_{AD}(t)\kappa]u_A^{\max}, \\ u_D^\ominus = -\text{sign}(Z_{AD}(t))u_D^{\max}, \end{cases} \quad (29)$$

where superscript max represents the maximal value.

3.3. Optimal Trajectories for the Attacker. In the attacker-target engagement, the optimal pursuit strategy for the attacker in equation (28) is

$$u_A^\ominus = \text{sign}(Z_{AT}(t))u_A^{\max}. \quad (30)$$

It is assumed that u_A^{\max} , u_T^{\max} , and u_D^{\max} satisfy $u_A^{\max} > u_T^{\max}$ and $u_A^{\max} > u_D^{\max}$ in the scenario. $\dot{Z}_{AT}(t)$ satisfies the following form:

$$\dot{Z}_{AT}(t) = t_{go}^{AT} [-\text{sign}(Z_{AT}(t))u_A^{\max} + \text{sign}(Z_{AT}(t))u_T^{\max}]. \quad (31)$$

The kill radius of the attacker is R ; $Z_{AT}(t)$ satisfies

$$Z_{AT}(t) + \int_t^{t_f^{AT}} [-\text{sign}(Z_{AT}(\xi))u_A^{\max} + \text{sign}(Z_{AT}(\xi))u_T^{\max}] (t_f^{AT} - \xi) d\xi = R. \quad (32)$$

The positive and negative pursuit boundary trajectories are given by

$$\begin{cases} Z_{AT}^\ominus(t_{go}^{AT}) = R - \frac{1}{2}(-u_A^{\max} + u_T^{\max})(t_{go}^{AT})^2, \\ -Z_{AT}^\ominus(t_{go}^{AT}) = -R + \frac{1}{2}(-u_A^{\max} + u_T^{\max})(t_{go}^{AT})^2. \end{cases} \quad (33)$$

Figure 2 presents the optimal pursuit trajectories. The positive and negative boundary trajectories are marked with triangles. In the engagement, the attacker uses the optimal pursuit guidance law, and the target uses the optimal evasion guidance law corresponding to equation (28). If $Z_{AT}(t)$ locates on the boundary trajectories, the final miss distance between the attacker and the target will be R . If $Z_{AT}(t)$ locates within the zone between the positive and negative boundary trajectories, the final miss distance between the attacker and the target will be less than R ; thus, the attacker can hit the target successfully. Conversely, the aircraft evades the attacker successfully.

The defender is launched from the target; thus, κ is always a positive value. Similarly, $\dot{Z}_{AD}(t)$ satisfies the following form:

$$\dot{Z}_{AD}(t) = t_{go}^{AD} [\text{sign}(Z_{AD}(t))u_A^{\max}\kappa - \text{sign}(Z_{AD}(t))u_D^{\max}]. \quad (34)$$

The kill radius of the defender is M ; $Z_{AD}(t)$ satisfies

$$Z_{AD}(t) + \int_t^{t_f^{AD}} [\text{sign}(Z_{AD}(\xi))u_A^{\max}\kappa - \text{sign}(Z_{AD}(\xi))u_D^{\max}] (t_f^{AD} - \xi) d\xi = M. \quad (35)$$

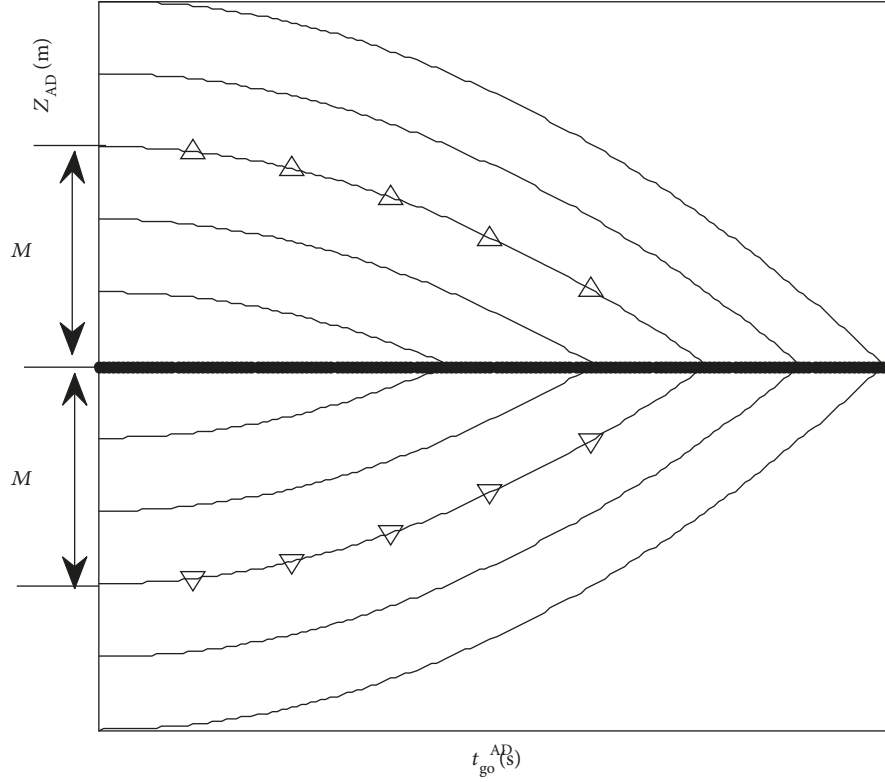


FIGURE 3: Optimal evasion trajectories.

The positive and negative evasion boundary trajectories are given by

$$\begin{cases} Z_{AD}^{\ominus}(t_{go}^{AD}) = M - \frac{1}{2}(u_A^{\max}\kappa - u_D^{\max})(t_{go}^{AD})^2, \\ -Z_{AD}^{\ominus}(t_{go}^{AD}) = -M + \frac{1}{2}(u_A^{\max}\kappa - u_D^{\max})(t_{go}^{AD})^2. \end{cases} \quad (36)$$

Figure 3 presents the optimal evasion trajectories under the condition that $u_A^{\max}\kappa > u_D^{\max}$. The positive and negative boundary trajectories are marked with triangles. In the engagement, the attacker uses the optimal evasion guidance law, and the defender uses the optimal intercept guidance law corresponding to equation (29). If $Z_{AD}(t)$ locates on the boundary trajectories, the final miss distance between the attacker and the defender will be M . If $Z_{AD}(t)$ locates without the zone between the positive and negative boundary trajectories, the final miss distance between the attacker and the defender will be larger than M ; thus, the attacker can evade the defender successfully. Conversely, the defender intercepts the attacker successfully.

It can be noted that if the signs of Z_{AT} and Z_{AD} are the same, the optimal strategies of the attacker are different in equations (28) and (29). It means that when the attacker pursues the target, it will approach the defender. Figure 4 shows the time evolution of the ZEMs for the situation in which the attacker evades the defender before the engagement time t_f^{AD} , then pursues the target. It is

shown that if the attacker evades the defender before t_f^{AD} , the absolute value of Z_{AT} will increase heavily, and it will go out of the zone between the positive and negative pursuit boundary trajectories easily. Thus, it is difficult for the attacker to pursue the target successfully after t_f^{AD} .

Figure 5 shows the time evolution of the ZEMs for the situation in which the attacker pursues the target in the total endgame phase. It is shown that the value of Z_{AD} will easily go in the zone between the positive and negative evasion boundary trajectories. Thus, the attacker can be intercepted easily by the defender because the attacker only pursues the target and ignores the defender.

3.4. Optimal Pursuit Strategy for the Attacker. If the attacker wants to win the game, the attacker needs to evade from the defender and pursue the target. Thus, the cost function is designed by

$$J = -\frac{1}{2}\alpha [Z_{AD}(t_f^{AD})]^2 + \frac{1}{2}\beta [Z_{AT}(t_f^{AT})]^2, \quad (37)$$

where α and β are nonnegative weights.

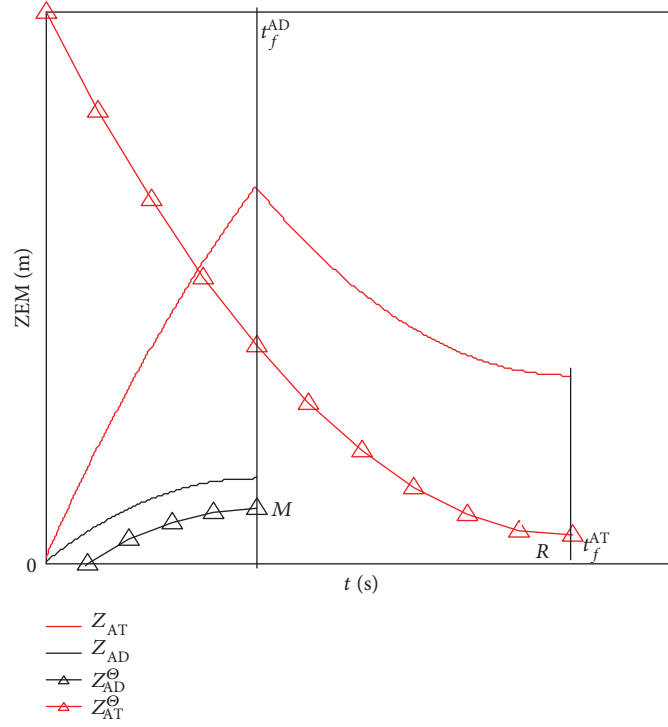
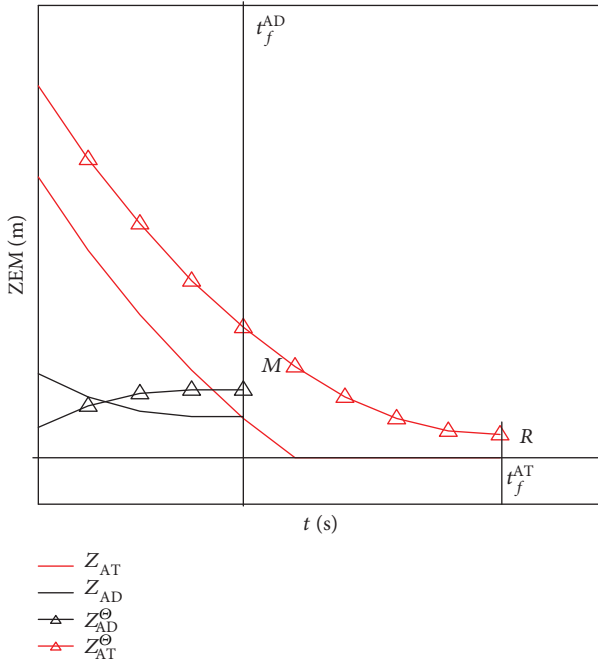

 FIGURE 4: Time evolution of the ZEMs for the attacker evading the defender before t_f^{AD} .


FIGURE 5: Time evolution of the ZEMs for the attacker pursuing the target in the total endgame phase.

TABLE 1: Initial parameters.

Parameters (unit)	Target	Attacker	Defender
Initial position (km)	(6, 2)	(0, 0)	(6, 2)
Initial course (deg)	5	0	7.5
Maximal acceleration (m/s^2)	50	180	70
Speed (m/s)	300	600	800

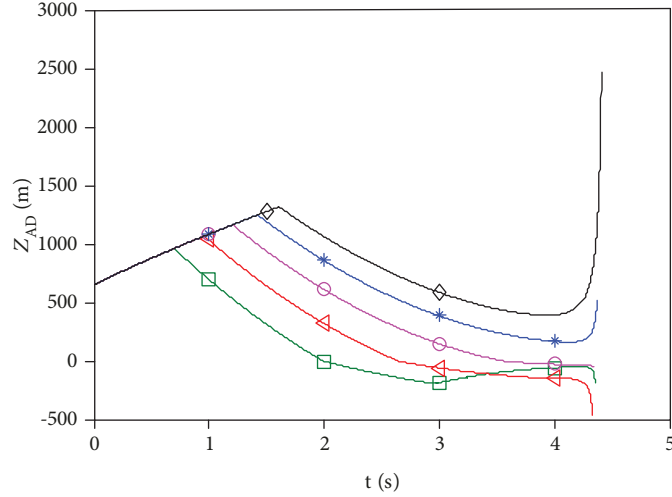
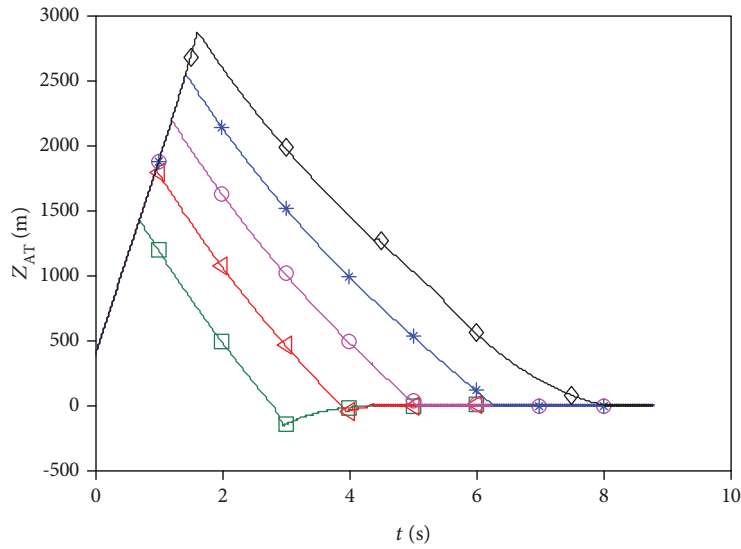
The Hamiltonian function of the problem is in the following form:

$$H = \lambda_1 \dot{Z}_{AD}(t) + \lambda_2 \dot{Z}_{AT}(t). \quad (38)$$

Parameters satisfy

$$\begin{cases} \dot{\lambda}_1 = -\frac{\partial H}{\partial Z_{AD}} = 0, \\ \lambda_1(t_f^{AD}) = \frac{\partial J}{\partial Z_{AD}(t_f^{AD})} = -\alpha Z_{AD}(t_f^{AD}), \\ \dot{\lambda}_2 = -\frac{\partial H}{\partial Z_{AT}} = 0, \\ \lambda_2(t_f^{AT}) = \frac{\partial J}{\partial Z_{AT}(t_f^{AT})} = \beta Z_{AT}(t_f^{AT}). \end{cases} \quad (39)$$

Substituting equations (39) and (20) into equation (38),

FIGURE 6: Time evolutions of $Z_{AD}(t)$.FIGURE 7: Time evolutions of $Z_{AT}(t)$.

we can obtain the following equation:

$$H = \left[\alpha Z_{AD} \left(t_f^{AD} \right) \Gamma(t) \kappa t_{go}^{AD} - \beta Z_{AT} \left(t_f^{AT} \right) t_{go}^{AT} \right] \times u_A \quad (40)$$

$$- \alpha Z_{AD} \left(t_f^{AD} \right) \Gamma(t) t_{go}^{AD} u_D + \beta Z_{AT} \left(t_f^{AT} \right) t_{go}^{AT} u_T.$$

The open-loop optimal strategies can be expressed as follows:

$$\begin{cases} u_A^\ominus = -\text{sign} \left[\alpha Z_{AD} \left(t_f^{AD} \right) \Gamma(t) t_{go}^{AD} \kappa - \beta Z_{AT} \left(t_f^{AT} \right) t_{go}^{AT} \right] u_A^{\max}, \\ u_T^\ominus = \text{sign} \left[Z_{AT} \left(t_f^{AT} \right) t_{go}^{AT} \right] u_T^{\max}, \\ u_D^\ominus = -\text{sign} \left[Z_{AD} \left(t_f^{AD} \right) \alpha \Gamma(t) t_{go}^{AD} \right] u_D^{\max}. \end{cases} \quad (41)$$

The close-loop optimal strategies of u_T^\ominus and u_D^\ominus are solved as follows:

$$\begin{cases} u_T^\ominus = \text{sign} \left[Z_{AT}(t) t_{go}^{AT} \right] u_T^{\max}, \\ u_D^\ominus = -\text{sign} \left[Z_{AD}(t) \alpha \Gamma(t) t_{go}^{AD} \right] u_D^{\max}, \end{cases} \quad (42)$$

where superscript max represents the maximal value.

The close-loop optimal strategy of the attacker is difficult to obtain. The open-loop optimal strategy is

$$u_A^\ominus = -\text{sign} \left[\alpha Z_{AD} \left(t_f^{AD} \right) \Gamma(t) t_{go}^{AD} \kappa - \beta Z_{AT} \left(t_f^{AT} \right) t_{go}^{AT} \right] u_A^{\max}. \quad (43)$$

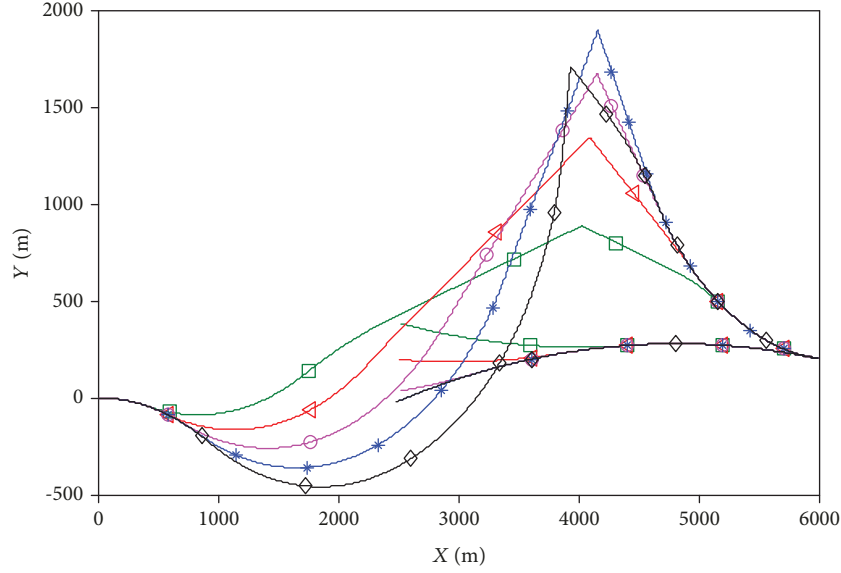


FIGURE 8: Time evolutions of trajectories.

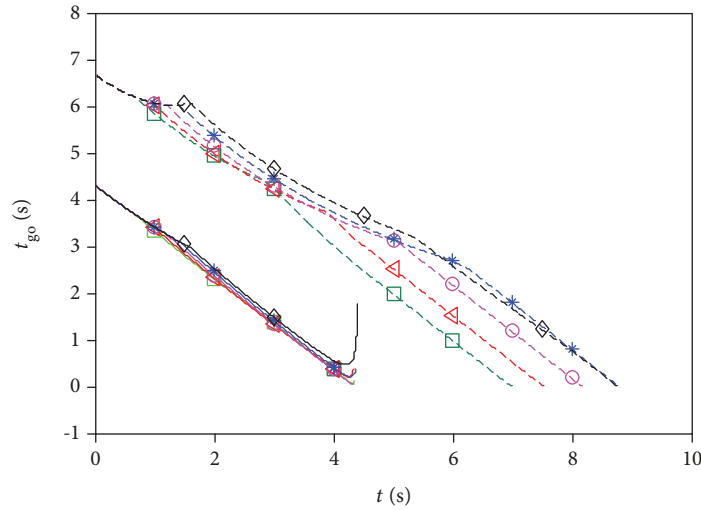


FIGURE 9: Time evolutions of time-to-go.

The strategy is designed for the attacker to evade from the defender and pursue the target as follows:

$$u_A^\ominus = \text{sign} \left[\alpha Z_{AD}(t) \Gamma(t) t_{go}^{AD} \kappa - \beta Z_{AT}(t) t_{go}^{AT} \right] u_A^{\max}. \quad (44)$$

Equation (44) can be rewritten as follows:

$$u_A^\ominus = \text{sign} \left[\frac{\alpha}{\beta} Z_{AD}(t) \Gamma(t) t_{go}^{AD} \kappa - Z_{AT}(t) t_{go}^{AT} \right] u_A^{\max}. \quad (45)$$

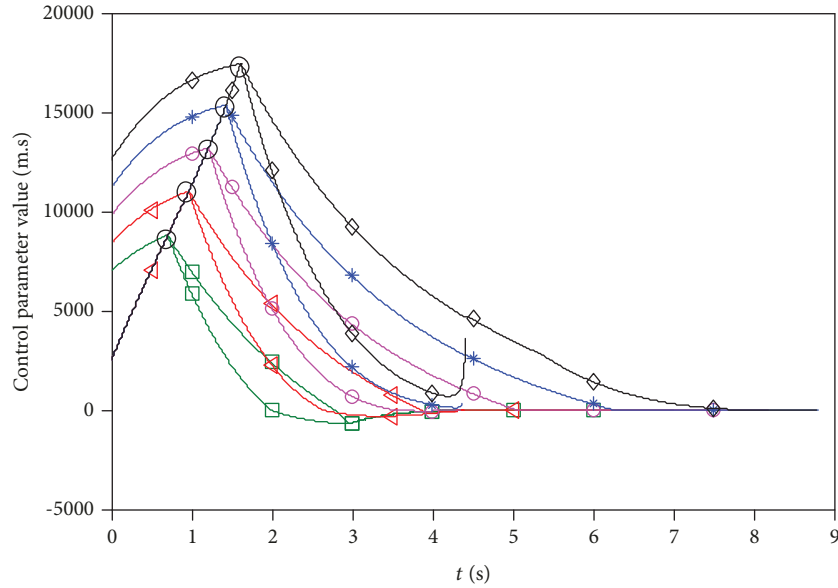
4. Nonlinear Simulation

The initial condition is shown in Table 1.

Figures 6, 7, 8, and 9 show the time evolutions of $Z_{AD}(t)$, $Z_{AT}(t)$, three players' trajectories, and time-to-go by using nonlinear simulation for different values of α/β . Figure 10

shows the values of the control parameters corresponding to $\alpha/\beta Z_{AD}(t) t_{go}^{AD} \kappa$ and $Z_{AT}(t) t_{go}^{AT}$. In the simulation phase, the initial line of sight is updated in real time, and t_f^{AD} and t_f^{AT} are replaced by t_{go}^{AD} and t_{go}^{AT} . The meaning of the lines for different values of α/β are shown in Figure 11. The engagement times and the miss distances are shown in Table 2.

It is shown that when the time approaches the engagement time t_f^{AD} , the absolute value of $Z_{AD}(t)$ increases substantially because at this time, the LOS changes quickly, and t_{go}^{AD} increases heavily. It is noted that at the initial time, $Z_{AD}(t)$ and $Z_{AT}(t)$ increase because at this time, the absolute value of $\alpha/\beta Z_{AD}(t) t_{go}^{AD} \kappa$ is bigger than that of $Z_{AT}(t) t_{go}^{AT}$, and the attacker tries to minimize the cost function. As time goes on, the absolute value of $Z_{AT}(t) t_{go}^{AT}$ increases more quickly,



○ Change points of control direction

FIGURE 10: Time evolutions of the control parameters of $\alpha/\beta Z_{AD}(t)t_{go}^{AD}\kappa$ and $Z_{AT}(t)t_{go}^{AT}$.

α/β value	$Z_{AD}(t)$ (Figure 6)	$Z_{AT}(t)$ (Figure 7)	Attacker trajectory Figure 8	Defender trajectory Figure 8	Target trajectory Figure 8	t_{go}^{AD} (Figure 9)	t_{go}^{AT} (Figure 9)	$\alpha/\beta \times Z_{AD}(t)t_{go}^{AD}\kappa$ value (Figure 10)	$Z_{AT}(t)t_{go}^{AT}$ value (Figure 10)
2.5	—□—	—□—	...□...	--□--	—□—	—□—	...□...	—□—	--□--
3	—△—	—△—	...△...	--△--	—△—	—△—	...△...	—△—	--△--
3.5	—○—	—○—	...○...	--○--	—○—	—○—	...○...	—○—	--○--
4	—◆—	—◆—	...◆...	--◆--	—◆—	—◆—	...◆...	—◆—	--◆--
4.5	—◇—	—◇—	...◇...	--◇--	—◇—	—◇—	...◇...	—◇—	--◇--

FIGURE 11: Meanings of the lines for different values of α/β .

and its influence on the cost function becomes greater. Thus, the control direction of the attacker changes, which leads to the decrease of $Z_{AD}(t)$ and $Z_{AT}(t)$. It can be concluded that the attacker can evade from the defender and hit the target by using the derived strategy through observing the trajectories, and results are shown in Figure 8 and Table 2.

5. Conclusion

The scenario in which the attacker attacks the active defense aircraft is investigated. In this scenario, the target evades the attacker, and the defender intercepts the attacker by using optimal guidance laws. The optimal

TABLE 2: Simulation results for different values of α/β .

α/β	Miss distance (m) (AD)	Miss distance (m) (AT)	t_f^{AT} (s)	t_f^{AD} (s)
2.5	47.464	0.235	6.9913	4.3632
3	132.881	0.183	7.5299	4.3645
3.5	32.875	0.389	8.1781	4.3622
4	141.523	0.062	8.7972	4.4023
4.5	318.687	0.045	8.7778	4.4392

one-to-one guidance law is derived for the attacker. If the attacker evades the defender by using the optimal evasion guidance law before t_f^{AD} , it will go out of the zone between the positive and negative pursuit boundary trajectories easily. Thus, it is difficult for the attacker to pursue the target successfully after t_f^{AD} . If the attacker pursues the target in the total endgame phase, the value of Z_{AD} will easily go in the zone between the positive and negative evasion boundary trajectories, and the attacker can be intercepted by the defender.

Thus, a new strategy is derived for the attacker to win the game in the active defense scenario. In this problem, the target evades from the attacker, and the defender intercepts the attacker by using the derived close-loop optimal strategies. Although the close-loop strategy is difficult to obtain by using the presented cost function for the attacker, an available strategy is designed for it based on the open-loop solution. The attacker can accomplish the task of evading from the defender and pursuing the target by using the derived strategy.

Data Availability

The data used to support the findings of this study are available from the corresponding author upon request.

Conflicts of Interest

The authors declare that they have no competing interests.

Acknowledgments

This work was cosupported by the National Natural Science Foundation of China (11672093) and the Shanghai Aerospace Science and Technology Innovation Foundation (SAST2016039).

References

- [1] P. Zarchan, "Tactical and strategic missile guidance," *Progress in Astronautics and Aeronautics*, vol. 219, pp. 11–29, 2007.
- [2] Z. Yang, H. Wang, D. Lin, and L. Zang, "A new impact time and angle control guidance law for stationary and nonmaneuvering targets," *International Journal of Aerospace Engineering*, vol. 2016, Article ID 6136178, 14 pages, 2016.
- [3] J. Ye, H. Lei, and J. Li, "Novel fractional order calculus extended PN for maneuvering targets," *International Journal of Aerospace Engineering*, vol. 2017, Article ID 5931967, 9 pages, 2017.
- [4] Y. Si and S. Song, "Three-dimensional adaptive finite-time guidance law for intercepting maneuvering targets," *Chinese Journal of Aeronautics*, vol. 30, no. 6, pp. 1985–2003, 2017.
- [5] Y. Zhang, S. Tang, and J. Guo, "An adaptive fast fixed-time guidance law with an impact angle constraint for intercepting maneuvering targets," *Chinese Journal of Aeronautics*, vol. 31, no. 6, pp. 1327–1344, 2018.
- [6] T. Wang, S. Tang, J. Guo, and H. Zhang, "Two-phase optimal guidance law considering impact angle constraint with bearings-only measurements," *International Journal of Aerospace Engineering*, vol. 2017, Article ID 1380531, 12 pages, 2017.
- [7] Z. Yang, H. Wang, and D. Lin, "Time-varying biased proportional guidance with seeker's field-of-view limit," *International Journal of Aerospace Engineering*, vol. 2016, Article ID 9272019, 11 pages, 2016.
- [8] S. S. Kumkov, S. L. Menec, and V. S. Patsko, "Solvability sets in pursuit problem with two pursuers and one evader," *IFAC Proceedings Volumes*, vol. 47, no. 3, pp. 1543–1549, 2014.
- [9] S. S. Kumkov, S. Le Ménéec, and V. S. Patsko, "Level sets of the value function in differential games with two pursuers and one evader. Interval analysis interpretation," *Mathematics in Computer Science*, vol. 8, no. 3-4, pp. 443–454, 2014.
- [10] J. Zhao and S. Yang, "Integrated cooperative guidance framework and cooperative guidance law for multi-missile," *Chinese Journal of Aeronautics*, vol. 31, no. 3, pp. 546–555, 2018.
- [11] X. Wei, Y. Wang, S. Dong, and L. Liu, "A three-dimensional cooperative guidance law of multimissile system," *International Journal of Aerospace Engineering*, vol. 2015, 8 pages, 2015.
- [12] J. Zeng, L. Dou, and B. Xin, "A joint mid-course and terminal course cooperative guidance law for multi-missile salvo attack," *Chinese Journal of Aeronautics*, vol. 31, no. 6, pp. 1311–1326, 2018.
- [13] R. Boyell, "Defending a moving target against missile or torpedo attack," *IEEE Transactions on Aerospace and Electronic Systems*, vol. AES-12, no. 4, pp. 522–526, 1976.
- [14] R. Boyell, "Counterweapon aiming for defense of a moving target," *IEEE Transactions on Aerospace and Electronic Systems*, vol. AES-16, no. 3, pp. 402–408, 1980.
- [15] J. Shinar and G. Silberman, "A discrete dynamic game modeling anti-missile defense scenarios," *Dynamics and Control*, vol. 5, no. 1, pp. 55–67, 1995.
- [16] I. Rusnak, "The lady, the bandits and the body guards - a two team dynamic game," in *Proceedings of the 16th world IFAC congress*, pp. 441–446, Prague, Czech Republic, July 2005.
- [17] A. Ratnoo and T. Shima, "Line-of-sight interceptor guidance for defending an aircraft," *Journal of Guidance, Control, and Dynamics*, vol. 34, no. 2, pp. 522–532, 2011.

- [18] T. Shima, "Optimal cooperative pursuit and evasion strategies against a homing missile," *Journal of Guidance, Control, and Dynamics*, vol. 34, no. 2, pp. 414–425, 2011.
- [19] O. Prokopov and T. Shima, "Linear quadratic optimal cooperative strategies for active aircraft protection," *Journal of Guidance, Control, and Dynamics*, vol. 36, no. 3, pp. 753–764, 2013.
- [20] J. F. Fisac and S. S. Sastry, "The pursuit-evasion-defense differential game in dynamic constrained environments," in *2015 54th IEEE Conference on Decision and Control (CDC)*, pp. 4549–4556, Osaka, Japan, December 2015.
- [21] D. W. Oyler, P. T. Kabamba, and A. R. Girard, "Pursuit-evasion games in the presence of obstacles," *Automatica*, vol. 65, no. 1, pp. 1–11, 2016.
- [22] S. Zhang, Y. Guo, and S. Wang, "Cooperative intercept guidance of multiple aircraft with a lure role included," *International Journal of Aerospace Engineering*, vol. 2018, Article ID 4126807, 15 pages, 2018.
- [23] S. Qilong, Q. Naiming, X. Zheyao, L. Yanfang, and Z. Yong, "An optimal one-way cooperative strategy for two defenders against an attacking missile," *Chinese Journal of Aeronautics*, vol. 30, no. 4, pp. 1506–1518, 2017.
- [24] E. Garcia, D. W. Casbeer, K. Pham, and M. Pachter, "Cooperative aircraft defense from an attacking missile," in *53rd IEEE Conference on Decision and Control*, pp. 2926–2931, Los Angeles, CA, USA, December 2014.
- [25] E. Garcia, D. W. Casbeer, and M. Pachter, "Active target defense differential game with a fast defender," in *2015 American Control Conference (ACC)*, pp. 3752–3757, Chicago, IL, USA, July 2015.
- [26] S. R. Kumar and T. Shima, "Cooperative nonlinear guidance strategies for aircraft defense," *Journal of Guidance, Control, and Dynamics*, vol. 40, no. 1, pp. 124–138, 2017.
- [27] Q. Sun, N. Qi, L. Xiao, and H. Lin, "Differential game strategy in three-player evasion and pursuit scenarios," *Journal of Systems Engineering and Electronics*, vol. 29, no. 2, pp. 352–366, 2018.
- [28] S. Rubinsky and S. Gutman, "Three-player pursuit and evasion conflict," *Journal of Guidance, Control, and Dynamics*, vol. 37, no. 1, pp. 98–110, 2014.
- [29] N. Qi, Q. Sun, and J. Zhao, "Evasion and pursuit guidance law against defended target," *Chinese Journal of Aeronautics*, vol. 30, no. 6, pp. 1958–1973, 2017.

